Stem Cell Reviews and Reports (2023) 19:2465–2480
https://doi.org/10.1007/s12015-023-10570-w

MSC-Derived Exosomes Ameliorate Intervertebral Disc Degeneration By Regulating the Keap1/Nrf2 Axis

Guangyu Xu[1] · Xiao Lu[1] · Siyang Liu[1] · Yuxuan Zhang[1] · Shun Xu[2] · Xiaosheng Ma[1] · Xinlei Xia[1] · Feizhou Lu[1,2] · Fei Zou[1] · Hongli Wang[1] · Jian Song[1] · Jianyuan Jiang[1]

Accepted: 24 May 2023 / Published online: 1 August 2023

Abstract

Bone marrow mesenchymal stem cell derived exosomes (BMSC-exos) are a crucial means of intercellular communication and can regulate a range of biological processes by reducing inflammation, decreasing apoptosis and promoting tissue repair. The process of intervertebral disc degeneration (IVDD) is accompanied by increased reactive oxygen species (ROS) because of a decrease in the expression of Nrf2, a critical transcription factor that resists excessive ROS. Our study demonstrated that BMSC-exos decreased ROS production by inhibiting Keap1 and promoting Nrf2 expression, attenuating the apoptosis, inflammation, and degeneration of nucelus pulposus (NP) cells. BMSC-exos promoted an increase in Nrf2 and nuclear translocation, while NF-κB expression was downregulated during this process. Additionally, the expression of antioxidative proteins was elevated after treatment with BMSC-exos. In vivo, we found more NP tissue retention in the BMSC-exos-treated group, along with more expression of Nrf2 and antioxidant-related proteins. Our findings demonstrated for the first time that BMSC-exos could restore the down-regulated antioxidant response system in degenerating NP cells by modulating the Keap1/Nrf2 axis. BMSC-exos could be used as an immediate ROS modulator in the treatment of intervertebral disc degeneration.

Keywords Nrf2 · Low back pain · Inflammation · Oxidative stress · Exosomes

Introduction

Low back pain is a global health problem with high morbidity rates, and it imposes a significant clinical and socioeconomic burden [1]. IVDD has been considered the main cause [2]. The physiological state of NP cells plays a major role in the progression of IVDD, while the loss of NP cells and decomposition of the extracellular matrix (ECM) substantially accelerate disc degeneration [3–6]. Additionally, increased inflammation and elevated ROS levels in NP cells often accompany the degenerative process [4, 7]. Recently, increasing evidences of an imbalance of excessive ROS and diminished antioxidant capacity in degenerating or ageing discs were reported [8, 9]. Since ROS is an important mediator of IVDD progression, improving the antioxidant capacity of NP cells is considered a promising therapeutic strategy for IVDD.

In mammals, transcription factor nuclear factor erythroid-2 related Factor 2 (Nrf2)-mediated resistance to oxidation and stress is a more conservative defence system to ensure intracellular homeostasis [10]. The abundance of intracellular Nrf2 is strictly regulated by Kelch-like ECH-associated protein 1 (Keap1), a redox-sensitive E3 ubiquitin ligase substrate adapter, which indicates that Keap1 promotes the ubiquitination of the Nrf2 protein, leading to proteasome-dependent degradation of Nrf2 [11, 12]. Inhibition of keap1 activity stabilizes Nrf2, facilitates its translocation to the nucleus, and then activates the defence network against abnormal ROS [11, 13]. In the intracellular

Gungayu Xu, Xiao Lu and Siyang Liu contributed equally.

✉ Jian Song
jsong16@fudan.edu.cn

✉ Jianyuan Jiang
jianyuanjiang@sina.com

Fei Zou
zoufei@huashan.org.cn

Hongli Wang
wanghongli0212@163.com

[1] Department of Orthopedics, Huashan Hospital, Fudan University, Shanghai 200040, China

[2] Department of Orthopedics, Shanghai Fifth People's Hospital, Fudan University, Shanghai 200240, China

antioxidant regulatory network, the main performers are heme-oxygenase-1 (HO-1) and NADP(H) quinone oxidoreductase 1 (NQO1), both of which are key downstream targets of Nrf2 [10, 11, 14]. Additionally, other antioxidant enzymes involved in scavenging ROS include superoxide dismutases (SODs), represented by SOD2 [14, 15]. Studies have shown that Nrf2 activation in degenerating discs can slow IVDD progression by mobilizing the intrinsic antioxidant capacity of cells, reducing excessive ROS [16–18]. With further understanding of the Keap1/Nrf2 signalling mechanism, this pathway has been implicated as a potential therapeutic direction for chronic and inflammatory diseases such as renal inflammation, pulmonary inflammation, and skin injury [19–21].

Exosomes are nanoscale vesicles secreted by cells and are rich in DNA, coding and noncoding RNA, and proteins [22]. The bilayer lipid membrane of exosomes allows them to penetrate cell membranes and transmit information across cells easily, further regulating the function of target cells and influencing disease progression [22, 23]. Previous studies have shown that exosomes can function as antioxidants and anti-inflammatory agents in neurological disorders, skin oxidation, and macrophage polarization by regulating the Keap1/Nrf2 axis [21, 24, 25]. In studies of IVDD, exosomes can suppress the activation of inflammatory mediators and NLRP3 inflammasome and thus reduce ROS level [26]. However, their cytoprotective role in collaboration with the Keap1/Nrf2 pathway has not been fully elucidated.

In this study, we demonstrated that bone marrow mesenchymal stem cell-derived exosomes (BMSC-exos) could mitigate the IVDD process by modulating the Keap1/Nrf2 signalling pathway to reduce excessive ROS both in vitro and in vivo. Additionally, a decrease in ROS could alleviate the inflammatory response, reduce the degradation of ECM and decrease apoptosis of NP cells, accompanied by inhibition of the NF-κB signalling pathway. These findings complement the exosome-mediated regulatory mechanisms that reduce oxidative stress in NP cells and deliver a new target for exosome-based IVDD therapy.

Materials and Methods

Isolation and Culture of Human NP Cells

The study was approved by the Ethics Committee of Huashan Hospital, Fudan University and the procedures followed were in accordance with the Helsinki Declaration of 1975. Patients enrolled in this study all provided informed consent. Normal NP tissues (with a Pfirrmann grade of II and III) were obtained from patients with Hirayama disease, and degenerative NP tissues were obtained from patients with cervical spondylotic myelopathy (with a Pfirrmann grade of IV and V) (Table S1). NP tissue (Pfirrmann grade of II) was fragmented and digested with collagenase type II enzyme (Invitrogen) at a concentration of 0.25 mg/ml for 8 h. After washing in PBS and centrifugation, isolated NP cells were cultured in Dulbecco's modified Eagle's medium (DMEM) containing 15% foetal bovine serum (FBS) and 1% dual antibiotics (Invitrogen). Cultured NP cells were then kept in a humid atmosphere at 37 °C. Every day, we replaced the entire medium with fresh medium. When no significant morphological changes between the primary and subsequent cells were confirmed, we used monolayer cultures of second-passage cells for experiments.

NP Cells Degeneration

H_2O_2 stimulation was used to induce cells degeneration. CCK-8 assay was used to assess the regulation of cell viability by different concentrations of H_2O_2 (100 μmol、250 μmol、500μmol、750 μmol) for twelve hours. Then, according to the optical density results of CCK-8 assays, a suitable concentration was selected for subsequent experiments.

CCK-8 Assay

Cell Counting Kit-8 (Beyotime, China) was applied to determine cell proliferation. NP cells were seeded in 96-well plates at 10^4 per well. After incubation with H_2O_2 with different concentration for twelve hours, the culture medium was removed. Then 10 μl of CCK-8 was added to every well. After 4 h of incubation, the 450 nm light absorption value was measured using a Diatek reader (DR-200bs).

Acquisition of BMSC-Exos

Human BMSCs were acquired from Procell (CP-H166) and amplified in DMEM. Cells of the second passage were used for subsequent experiments. To detect cellular signature markers, the positive expression of CD73, CD90 and CD105 and negative expression of CD34 and CD45 in MSCs were profiled using flow cytometry. (BD FACSCalibur, USA). Next, we replaced the culture medium with 10% FBS, which was centrifuged at 100,000 × g at 4 °C for 16 h to remove the original exosomes. After 2 days, the conditioned medium was harvested and centrifuged at 3,000 × g for 15 min at 4 °C. Next, we separated BMSC-exos from the medium using a Total Exosome Isolation ExoQuick PLUS Exosome Purification Kit (System Biosciences, USA). After that, the MSC-exos were purified and suspended in particle-free PBS and stored at -80 °C.

Identification and Uptake of BMSC-Exos

We chose transmission electron microscopy (TEM) to document the existence and morphology of exosomes. ZetaView was used to measure the size distribution and concentration. Additionally, western blotting was used to confirm the surface markers (positive expression of CD63 and CD81 and negative expression of β-actin).

We incubated purified BMSC-exos with PKH26 (Sigma-Aldrich, USA) for 5 min. Before suspension in basal medium and incubation with NP cells for 3 h at 37 °C, MSC-exos were washed twice in PBS and centrifuged at 120,000 g for 90 min. We stained nuclei with 4′,6-diamidino-2-phenylindole (DAPI) (Beyotime, China). Next, immunofluorescence staining was used to measure the uptake of labelled particles by NP cells.

I Vitro Effects of BMSC-Exos on Degenerated NP Cells

Degenerated NP cells were incubated with 200 μl of BMSC-exos (8.8×10^{10} particles/ml) for eight hours to ensure the incorporation of exosomes into NP cells (H_2O_2 + BMSC-exos group). Each well in a six-well plate has approximately 1×10^5 cells, which makes 1.8×10^5 exosomes per cell. On the other hand, the controlled groups were treated with same volume of PBS (H_2O_2 group) or normal NP cells (without H_2O_2 treatment). ML385 (5μmol), a specific Nrf2 inhibitor, was used to investigate the role of Nrf2 under the treatment of BMSC-exos.

Western Blotting

Western blotting was performed based on a standard protocol. Briefly, total protein was extracted using RIPA buffer and 1 mM PMSF (AS1006, ASPEN). A BCA protein kit (AS1086; ASPEN) was applied to measure the protein concentration. Proteins were separated by SDS–PAGE and transferred to PVDF membranes (Millipore). Before incubation with primary antibodies, the membranes were blocked with 5% nonfat milk. The primary antibodies were as follows: Adamts5 (1:300; ab41037), IL-1β (1:500; ab9722), Caspase-3 (1:500; ab44976), Aggrecan (1:500; ab3778), Keap1 (1:1000; ab227828), NQO1 (1:5000; ab80588) (Abcam, UK), MMP13 (1:1000; 18165-1), IL-6 (1:1000; 66146-1), HO-1 (1:2000; 27282-1), SOD2 (1:2000; 24127-1), Capase-7 (1:500; DF6441) (Affbiotech, USA), CollagenII (1:500; sc-52,658) (Santa, USA), Nrf2 (1:500; #12,721), p-IκBa (1:500; #2859), IκBa (1:1000; #4812), NF-κB p65 (1:2000; #8242) (CST, USA). After the incubation with corresponding secondary antibodies, the proteins were visualized and analysed by AlphaEaseFC Software (Alpha Innotech, USA). GAPDH protein was used for normalization.

Quantitative Real-Time PCR

TRIpure reagent (ELK Biotechnology) was applied to extract total RNA from cultured cells or tissues according to the manufacturer's instructions. The following primers were Please used:

TNF-α, forward 5' CATCATCCCTGCCTCTACTGG 3', reverse 5' GTGGGTGTCGCTGTTGAAGTC 3'; IL-1β, forward 5' CTGTAGCCCATGTTGTAGCAAAC 3', reverse 5' TGAAGAGGACCTGGGAGTAGATG 3'; IL-6, forward 5' ACTGGCAGAAAACAACCTGAAC 3', reverse 5' TTGTACTCATCTGCACAGCTCTG 3'; Keap1, forward 5' CCAATGCTGACACGAAGG AT 3', reverse 5' ATACAGTTGTGCAGGACGCAG 3'; Nrf2, forward 5' CAGTCAGCGACGGAAAGA GTA 3' reverse 5' CTGGGAGTAGTTGGCAGATCC 3'; HO-1, forward 5' GCCAGCAACAAAGTGCAA GA 3', reverse 5' TAAGGACCCATCGGAGAAGC 3'; NQO1, forward 5' TGGTGGAGTCGGACCTCT ATG 3', reverse 5' CATGGCAGCGTAAGTGTAAGC 3'; SOD2, forward 5' GTTTAAGGAGAAGCTGAC GGC 3', reverse 5' AGGTAGTAAGCGTGCTCCCAC 3'; GAPDH, forward 5' CATCATCCCTGCCTCTAC TGG 3', reverse 5' GTGGGTGTCGCTGTTGAAGTC 3'. GAPDH was used for normalization.

Senescence-Associated β-Galactosidase Staining

A SA-β-Gal kit (Beyotime, China) was used for senescence-associated β-galactosidase staining. One millilitre of β-galactosidase staining fixative was added to the 6-well plate at room temperature for 10 min. After incubation with staining solution for 2 h, microscopic fields were observed under a BX53 microscope (Olympus, Japan).

Flow Cytometry Analysis

An Annexin V-FITC Apoptosis Detection Kit (Beyotime, China) was applied to detect apoptosis. After collection from a six-well plate, the cells were centrifuged at 300 g for 5 min and resuspended in 300 μl of 1× binding buffer. After 15–20 min of incubation with 5 μl of Annexin V-FITC and 5 μl of PI, the cells were added with 200 μl bonding buffer and immediately measured using a FACS Calibur flow cytometer (BD Bioscience, USA).

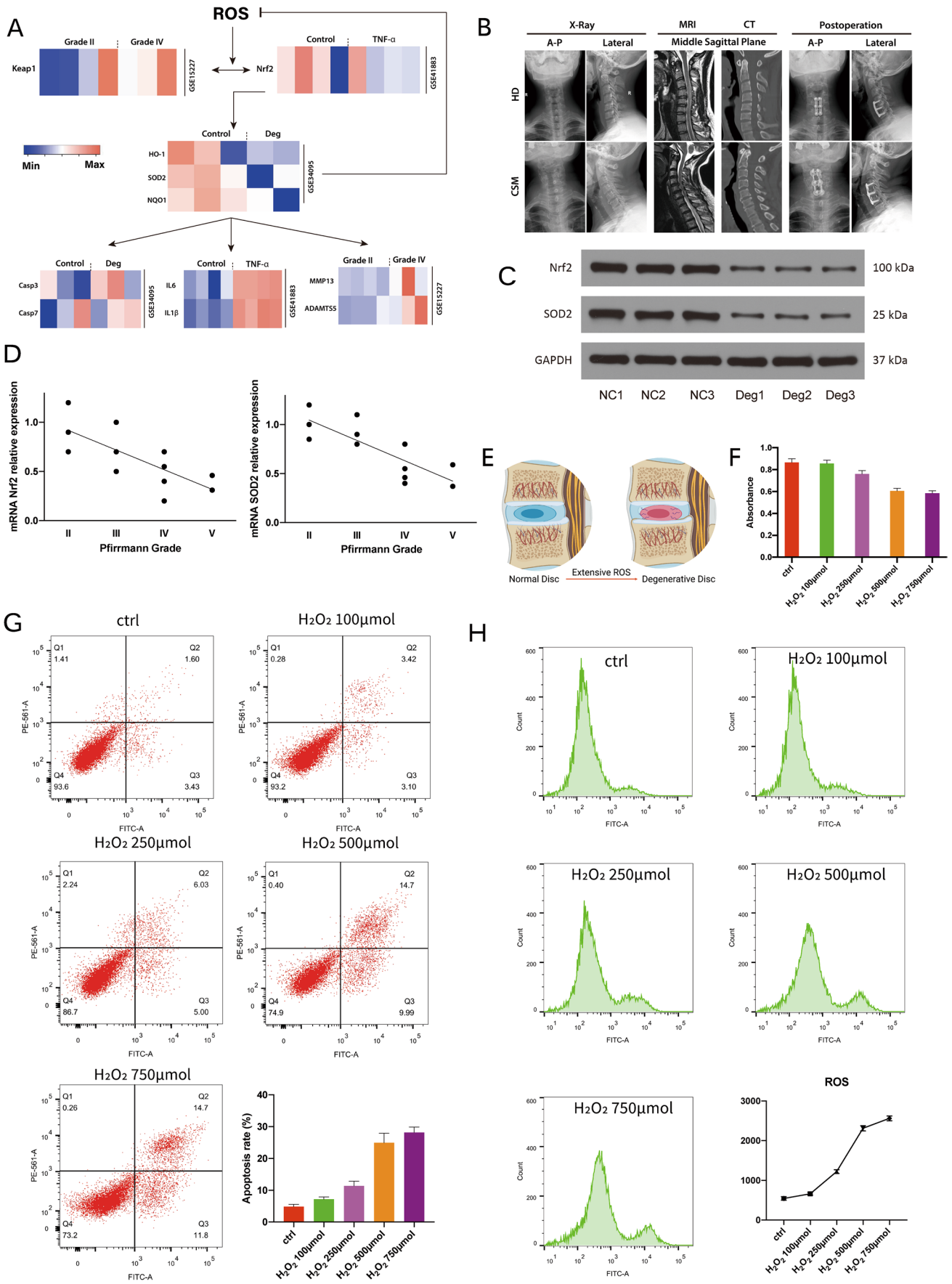
A
ROS
Grade II
Grade IV
Keap1
GSE15227
Nrf2
Control
TNF-α
GSE41883
Min
Max
Control
Deg
HO-1
SOD2
NQO1
GSE34095
Control
Deg
Casp3
Casp7
GSE34095
Control
TNF-α
IL6
IL1β
GSE41883
Grade II
Grade IV
MMP13
ADAMTS5
GSE15227
B
X-Ray
MRI
CT
Postoperation
A-P
Lateral
Middle Sagittal Plane
A-P
Lateral
HD
CSM
C
Nrf2
SOD2
GAPDH
100 kDa
25 kDa
37 kDa
NC1
NC2
NC3
Deg1
Deg2
Deg3
D
mRNA Nrf2 relative expression
1.0
0.5
0.0
II
III
IV
V
Pfirrmann Grade
mRNA SOD2 relative expression
1.0
0.5
0.0
II
III
IV
V
Pfirrmann Grade
E
Normal Disc
Extensive ROS
Degenerative Disc
F
Absorbance
1.0
0.8
0.6
0.4
0.2
0.0
ctrl
H2O2 100μmol
H2O2 250μmol
H2O2 500μmol
H2O2 750μmol
G
ctrl
Q1 1.41
Q2 1.60
Q4 93.6
Q3 3.43
H2O2 100μmol
Q1 0.28
Q2 3.42
Q4 93.2
Q3 3.10
H2O2 250μmol
Q1 2.24
Q2 6.03
Q4 86.7
Q3 5.00
H2O2 500μmol
Q1 0.40
Q2 14.7
Q4 74.9
Q3 9.99
H2O2 750μmol
Q1 0.26
Q2 14.7
Q4 73.2
Q3 11.8
PE-561-A
FITC-A
Apoptosis rate (%)
40
30
20
10
0
ctrl
H2O2 100μmol
H2O2 250μmol
H2O2 500μmol
H2O2 750μmol
H
ctrl
H2O2 100μmol
H2O2 250μmol
H2O2 500μmol
H2O2 750μmol
Count
FITC-A
ROS
3000
2000
1000
0
ctrl
H2O2 100μmol
H2O2 250μmol
H2O2 500μmol
H2O2 750μmol

◂**Fig. 1** Nrf2 was downregulated in IVDD patients and was accompanied by ROS-induced apoptosis in NP cells. **a** Heatmap showed different mRNA expression in non-degenerated and degenerated discs based on GSE15227, GSE41883, and GSE34095. (http://www.heatmapper.ca/expression/). **b** Representatives of X-rays, MR imaging and CT scans in patients with Hirayama disease (HD) and cervical spondylotic myelopathy (CSM). **c** Nrf2 and SOD2 were downregulated in degenerated discs in western blot assays. **d** The relationship between mRNA level of Nrf2 and SOD2 and Pfirrmann grade of discs using qPCR method. **e** The imbalance of extensive ROS and antioxidant proteins resulted in disc degeneration. **f** CCK-8 test of NPCs under different concentrations of H_2O_2. **g** Flow cytometry of apoptosis of NPCs under different concentrations of H_2O_2. **h** Flow cytometry of ROS of NPCs under different concentrations of H_2O_2. (Data were shown by mean ± SD, $n = 3$)

ROS Measurement

We used a ROS detection kit (Beyotime, China) to measure the overall intracellular ROS levels. DCFH-DA was diluted with serum-free culture medium at a 10 μmol/L concentration. We then added 1 ml of the diluted solution and incubated the cells with it for 20 min shielded from light. After washing with PBS, the sample was observed under a microscope or detected by flow cytometry.

RNA Interference

Short interfering RNA was used to knockdown Keap1. Si-RNA against Keap1 (si-Keap1) was synthesized by GenePharma (Shanghai, China) and transfected with Lipofectamine 2000 (Invitrogen). The si-Keap1 sequences were as follows: si-Keap1-1, 5'-GGCGAATGATCACAGCAAT-3'; si-Keap1-2, 5'-GCTACGATGTGGAAACAGA-3'; si-Keap1-3, 5'-GACAAACCGCCTTAATTCA-3'. After verifying the high silencing efficiency, NP cells were then used in subsequent experiments.

Immunofluorescence Analysis

NP cells were fixed in 4% paraformaldehyde. After permeabilization with Triton X, the slides were blocked with bovine serum for 2 h. Next, anti-8-OHdG (Abcam, UK), anti-Keap1, and anti-Nrf2 (PTG, USA) were incubated overnight at 37 °C. The slides were then washed with PBS 3 times before the corresponding secondary antibodies were added. Next, DAPI was used to stain cell nuclei. Then the images were captured by an immunofluorescence microscope (Olympus, Japan) and quantified by Image J software (NIH, USA).

TUNEL Assay

First, 4% paraformaldehyde was used to fix NP cells. Next, we used Triton X-100 in PBS for 10 min for permeabilization. After washing with PBS, the cell samples were subjected to the Cell Death Detection kit (Roche, Switzerland) according to the manufacturer's protocol. After that, DAPI was used to stain cell nuclei.

SD Rats of the IVDD Model

The animal experiments were conducted in accordance with the protocol of the Animal Experimentation Committee of Fudan University. Thirty-two female SD rats (adult, 200–250 g) were purchased from Charles River (Zhejiang, China) and housed in the Center for Animal Experiments of Fudan University (Shanghai, China). AAV-2 was synthesized by Zolgene (Fuzhou, China). The concentrations of Nrf2-shRNA and Keap1-shRNA were 1.3×10^{12} vg/ml. The animals were randomized to four groups (8 rats for each group): the IVDD group (PBS injection), MSC-exo group, MSC-exo + aav-siNrf2 group, and MSC-exo + aav-siNrf2 + aav-siKeap1 group. The tail disc of Co7-8 was selected for the punctured IVDD model using a 33G needle (Hamilton, Switzerland) for 30 s after anaesthesia with 2% pentobarbital sodium (40 mg/kg). The needle was punctured vertically through the skin and through the contralateral annulus fibrosus. Next, according to the different groupings, the discs were injected with exosomes (2 μL) or aav-2 vectors (2 μL). After the puncture, the rats were housed in a quite environment with accessible food and water.

MRI and X-ray Examination

Four weeks after injection, the rats were anaesthetized again for radiological evaluation. The discs were evaluated according to Pfirrmann grading using a 3.0T MR scanner (Siemens, Germany). X-rays were also obtained to evaluate the disc height (Philips, Netherlands). Disc height index (DHI) was then calculated for each disc. Three orthopaedic surgeons assessed the MRI grading on T2-weighted images and DHI% on X-ray images.

Histological Analysis

After intraperitoneal injection of an overdose of anaesthetics, the rats were sacrificed for NP tissues. The discs were fixed in 10% formalin for 7 days, followed by decalcification in EDTA for 21 days. Afterwards, the tissues were embedded in paraffin and sliced into 5 mm sections to perform HE and safranin-O staining. Then the disc was assessed with a histological scale for grading [27].

Statistical Analysis

Triplicate experiments were performed and the data were expressed as means ± 95%CI. Kolmogorov-Smirnov test was applied to assessed the normality of the parameters.

We then used unpaired two-tailed Student's t test for statistical analysis between two groups and one-way ANOVA for multiple group comparisons. All the data were analysed using Prism version 8.0 (La Jolla, USA) software. For all analyses, differences were considered statistically significant when $P < 0.05$.

Results

Downregulation of Antioxidants in IVDD and H_2O_2 Induced ROS Upregulation and Apoptosis

Expression of related antioxidants was identified in the GEO database (Fig. 1a). The degenerated group showed the downregulation of Nrf2, HO-1, NQO1, and SOD2 and upregulation of Keap1 along with inflammation and ECM degeneration. To further validate the expression level of antioxidants in IVDD, we evaluated six pairs of patients with cervical spondylotic myelopathy as the degenerated group and Hirayama disease as the control (Fig. 1b). Western blot analysis demonstrated the downregulation of antioxidants (Nrf2 and SOD2) (Fig. 1c), which was in accordance with qPCR results (Fig. 1d). The results confirmed the imbalance of antioxidants and ROS in the IVDD group (Fig. 1d and e). Next, different levels of H_2O_2 were used to treat NP cells for 12 h to simulate the degenerated environment. The CCK-8 assay and flow cytometry of apoptosis showed that the cell proliferation capacity decreased with increasing H_2O_2 concentration (Fig. 1f and g). Next, DCF was also detected by flow cytometry to evaluate ROS levels (Fig. 1h). All the results verified the apoptosis and ROS upregulation induced by H_2O_2. Since cell proliferation was markedly affected by H_2O_2 at a dose of 500 umol, we chose this dose for the following experiments.

Identification of MSC-Exos and Intake by NPC

Flow cytometry was used to identify the surface markers of BMSCs that were positive for CD73, CD90, and CD105 and negative for CD34 and CD45 (Fig. 2a and b). According to western blot results, the nanoparticles extracted from BMSCs were rich in CD63 and CD81 and lacked β-actin (Fig. 2c). (Fig. 2d). Furthermore, these particles presented a spherical shape under TEM and the diameter mainly ranged from 50 to 200 nm (Fig. 2d and e). Next, PKH-26 was used to label exosomes, and the incubation results showed that BMSC-exos were absorbed by NPCs over time (Fig. 2f and g).

BMSC-Exos Inhibit Excessive ROS, Accompanied by Reduced Inflammation, Degradation of ECM and Apoptosis

We then explored the effect of exosomes in NPCs under excessive ROS. Immunofluorescence results showed a decrease ROS in response to BMSC-exos (Fig. 3a). Because aging cells are less resistant to oxidative stress, we confirmed cellular senescence caused by excessive ROS and the antagonistic effect of exosomes using SA-b-Gal staining (Fig. 3b). Immunofluorescence of 8-Hydroxy-1,2 deoxyguanosine (8-OHdG), which is a symbol of DNA damage caused by ROS, again confirmed that BMSC-exos reduced cellular senescence under excessive ROS (Fig. 3c and d). Afterwards, the results of inflammatory agents such as TNF-α, IL-1β, and IL-6 by qPCR and flow cytometry demonstrated that BMSC-exos had a positive effect on reducing inflammation and apoptosis (Fig. 3e, f). To further investigate the effect of exosomes on the synthesis and degradation of ECM, MMP13, Adamts5, Collagen II, and Aggrecan were measured by western blotting (Fig. 3g, h). As expected, BMSC-exos reduced ROS-induced degeneration. Taken together, these data demonstrated that exosomes restored ROS-induced aging, accompanied by reduced inflammation, degradation of ECM and apoptosis of NP cells.

BMSC-Exos Increase the Expression and Nuclear Translocation of Nrf2 and Decrease the Expression of NF-κB

The aforementioned effects revealed that BMSC-exos could relieve H_2O_2-induced ROS and alleviate NP cell degeneration. Because the Keap1/Nrf2 axis is a key pathway in response to oxidative stress, we wondered whether exosomes exerted their effect by regulating it. After prolonged incubation with H_2O_2, the expression of Keap1 increased, and the expression of Nrf2 decreased slightly (Fig. 4a). Correspondingly, the expression of antioxidative stress-related proteins showed a decreasing trend (Fig. 4a). Next, we examined the expression of Keap1 and Nrf2 by immunofluorescence, which showed that excessive ROS triggered a rise in Keap1 expression and a decrease in Nrf2 expression (Fig. 4b, c). Interestingly, with BMSC-exos treatment, the adverse effect of H_2O_2 was offset (Fig. 4a-c). Western blot analysis showed that BMSC-exos significantly promoted the intranuclear translocation of Nrf2 (Fig. 4d). Next, we examined NF-κB expression, which has been implicated in the transcriptional regulation of ROS-induced inflammation. Not surprisingly, after incubation with H_2O_2, the nuclear translocation of NF-κB increased, accompanied by a significant increase in IκBα phosphorylation (Fig. 4d-f). Remarkably, the addition of

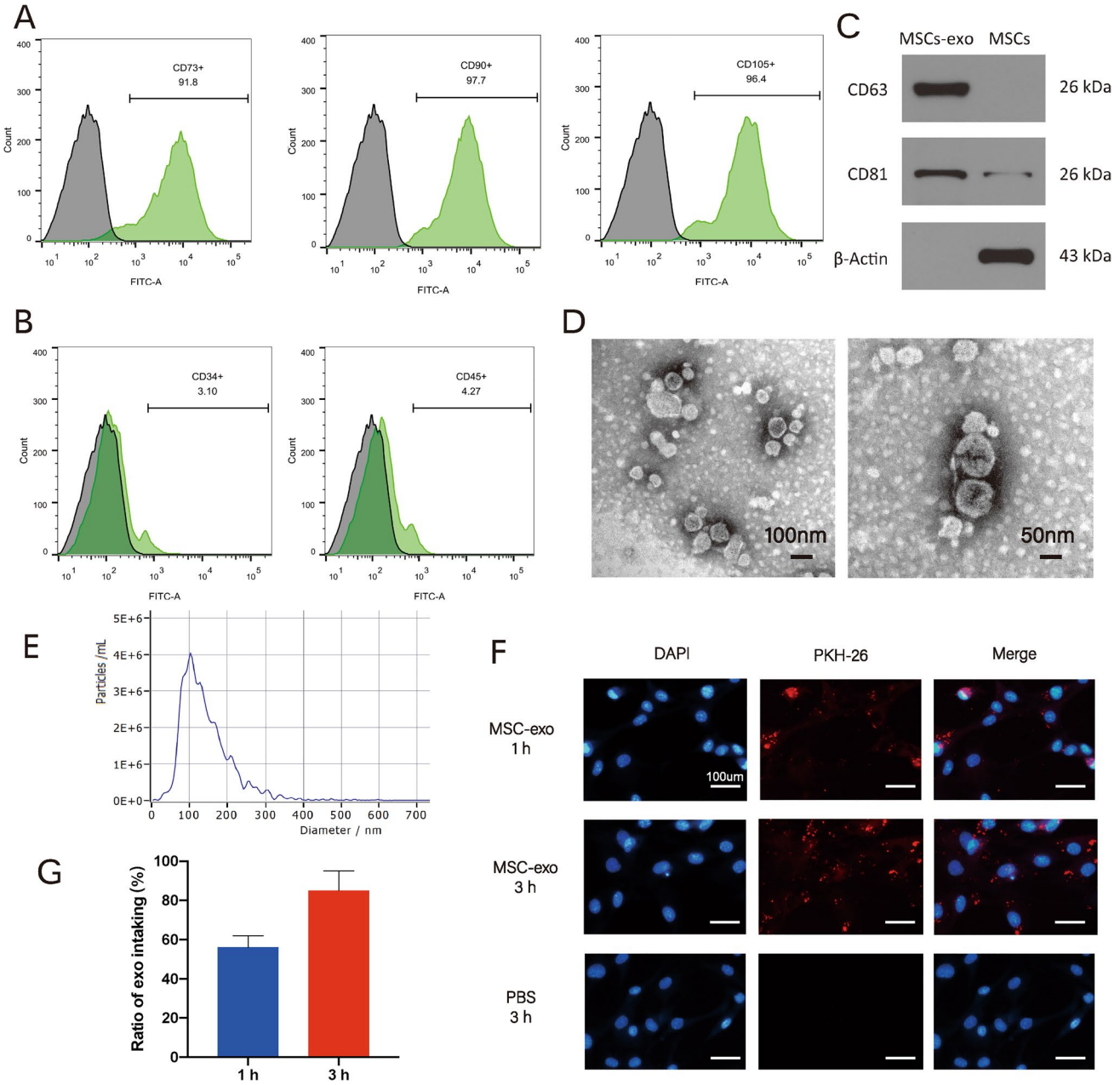

Fig. 2 Identification of BMSC-exos and the uptake of it by NPCs. **a** Positive surface markers of BMSC identified by flow cytometry (CD73, CD90, CD105). **b** Negative surface markers of BMSC identified by flow cytometry (CD34, CD45). **c** Western bolt assays of representative surface markers of BMSC-exos. **d** Morphology of BMSC-exos monitored by TEM (scale bar: left, 100 nm; right, 50 nm). **e** Particle size determined by a Zeta View nanoparticle tracker. X-axis showed the particle diameter while Y-axis showed the concentration of particles in the sample. **f** Immunofluorescence images of PKH26-labled BMSC-exos internalized by NPCs (scale bar, 100 μm). **g** Ratio of BMSC-exos intaking by NPCs. (Data were shown by mean ± SD, $n = 3$)

exosomes reversed the activation of NF-κB (Fig. 4d-f). We then used si-Keap1 to further confirm that BMSC-exos exerted antioxidative effects by regulating Keap1 and that Keap1 inversely regulated Nrf2 (Fig. 4g). Western blot assays demonstrated that si-Keap1 could upregulate Nrf2 expression and that exosomes helped to further reinforce this effect (Fig. 4h). Similarly, the expression of proteins that responded to ROS, such as HO-1, NQO1, and SOD2, showed the same results (Fig. 4i). These evidences together indicated that Keap1 was a negative regulator of Nrf2 and BMSC-exos exerted their anti-ROS effect by regulating Keap1 expression.

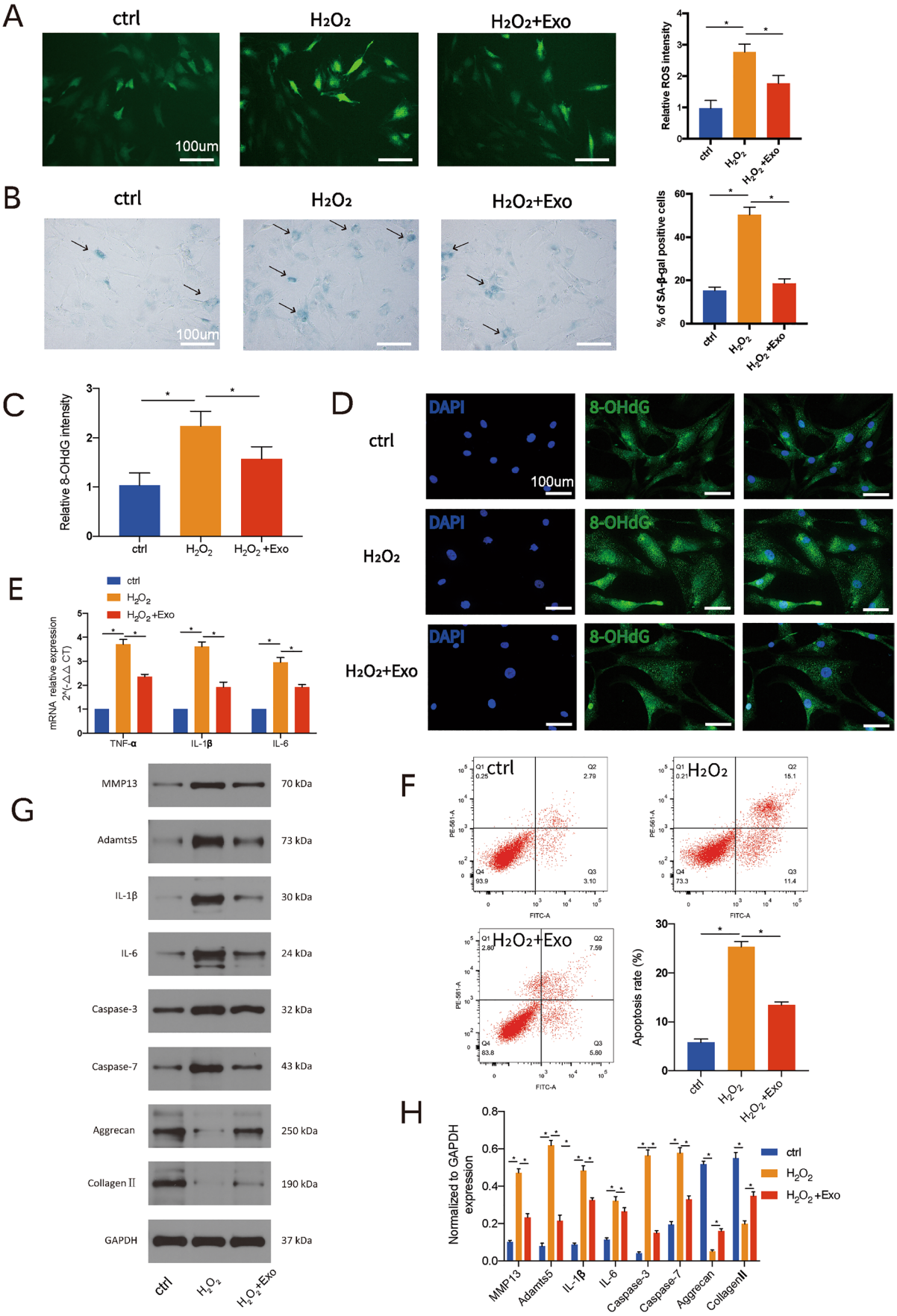
A
ctrl
H2O2
H2O2+Exo
100um
Relative ROS intensity
B
% of SA-β-gal positive cells
C
Relative 8-OHdG intensity
D
DAPI
8-OHdG
E
mRNA relative expression 2^(-ΔΔ CT)
TNF-α
IL-1β
IL-6
F
Apoptosis rate (%)
G
MMP13
Adamts5
IL-1β
IL-6
Caspase-3
Caspase-7
Aggrecan
Collagen II
GAPDH
70 kDa
73 kDa
30 kDa
24 kDa
32 kDa
43 kDa
250 kDa
190 kDa
37 kDa
H
Normalized to GAPDH expression

◂**Fig. 3** BMSC-exos inhibited excessive ROS, accompanied by reduced inflammation, degradation of ECM and apoptosis. **a** Immunofluorescence of 2′,7′-dichlorodihydrofluoroscein diacetate (DCF) to examine ROS level (scale bar, 100 μm). **b** SA-β-gal staining to determine cell senescence (scale bar, 100 μm). **c**-**d** Immunofluorescence of 8-OHdG to determine DNA damage by ROS (scale bar, 100 μm). **e** qPCR of mRNA levels of TNF-α, IL-1β, and IL-6 in each group. **f** Flow cytometry of apoptosis rate in each group. **g**-**h** BMSC-exos reversed the apoptosis, inflammation, and ECM degradation of H_2O_2. (Data were shown by mean ± SD, $n = 3$, $^*p < 0.05$)

Blockage of Nrf2 Abrogates the Anti-Inflammatory, Anti-Apoptotic, and Anti-ECM Degradation Effects of BMSC-Exos Under Oxidative Stress

To investigate the critical anti-ROS ability of Nrf2, we used the specific Nrf2 antagonist ML385 in subsequent experiments. The H_2O_2 group alone was considered a positive control group. Inhibition of Nrf2 reversed the reduction of ROS by BMSC-exos, while silencing of Keap1 restored the effect of BMSC-exos again (Fig. 5a). These findings implied that Nrf2 mediated at least some therapeutic advantage of BMSC-exos. Next, we used flow cytometry to examine the relationship between apoptosis and Nrf2, the result of which was the same with TUNEL staining (Fig. 5b and d). Treatment with ML385 contributed to a high rate of apoptosis, and the addition of si-Keap1 diminished the influence of ML385. Because Nrf2 plays an important role in anti-ROS, we used qPCR to investigate the mRNA levels of HO-1, NQO1, and SOD2. As expected, Nrf2 inhibition decreased the transcription of anti-ROS-related genes (Fig. 5c). Next, we applied western blots to examine the expression of inflammation-, apoptosis-, and ECM degradation-related genes (Fig. 5e, f). The results were consistent with the above. Finally, we used String to construct a protein interaction network in which Nrf2 was at the core (Fig. 5g).

BMSC-Exos Activate Nrf2 in Vivo to Alleviate IVDD in a Rat Model

To further confirm its role in regulating Keap1/Nrf2 pathway in vivo to alleviate IVDD, we first used a needle puncture model in rat tails to model the IVDD process. Adeno-associated virus 2 (AAV-2) carrying a gene-interfering sequence was injected into selected rat discs. Depending on the different treatments, the rats were divided into the puncture group, BMSC-exos group, si-Nrf2 + BMSC-exo group, and si-Keap1 + siNrf2 + BMSC-exo group. The Pfirrmann grade of the intervertebral disc was assessed by MRI four weeks after injection. Discs in the BMSC-exos group and si-Keap1 + siNrf2 + BMSC-exo group were significantly lower in Pfirrmann grading than those in the puncture group and si-Nrf2 + BMSC-exo group (Fig. 6a). The disc height index (DHI) in X-ray showed the same results (Fig. 6b). For histological evaluation, we used HE and Safranin-O staining to compare the intervertebral discs, which showed better preserved NP tissue in the BMSC-exos group than in the puncture group (Fig. 6c-e). We also used TUNEL staining to assess the rate of apoptosis in NP cells (Fig. 6f and g). Consequently, the ratio of DAB-positive cells in the puncture group and si-Nrf2 + BMSC-exo group was higher than that in the other groups, indicating that Nrf2 was a key mediator in exosome-induced recovery and suggesting the negative role of Keap1 in the degeneration process. Additionally, the results of western blots further demonstrated the increased expression of Nrf2 in vivo together with the increased expression of Collagen II and decreased expression of MMP13 and Caspase-3 (Fig. 6h and i). Collectively, these results confirmed that BMSC-exos could activate the Keap1/Nrf2 axis, restraining apoptosis and reducing inflammation and ECM degradation in vivo.

Discussion

Treatment strategies for IVDD mainly include enhancing synthesis of ECM, releasing pro-anabolic factors and inhibiting the degenerative microenvironment (including ROS) [28]. MiR-499a-5p and circRNA_104670 have been demonstrated to play a critical role in the balance between anabolism and catabolism of the ECM [6, 29]. Melatonin have also been demonstrated to inhibit ECM remodeling via PI3K-Akt pathway [30]. As for degenerative environment, previous studies have demonstrated that ROS plays a significant role in the development of IVDD [7, 31]. ROS are toxic but also serve as signalling molecules [32]. ROS can influence the activation of many signalling pathways and then modulate oxidative stress networks reversely. However, as cells age, the intracellular antioxidant capacity tends to diminish and thus it is difficult for cells to resist endogenous oxidative stress [8]. Macroscopically, increased ROS and disease progression are positively correlated in tissues [8, 33]. Redox imbalance is often correlated with inflammatory responses, disturbances in extracellular matrix metabolism and, in general, the promotion of cell apoptosis [34, 35]. Thus, factors controlling this pathway may be appealing molecular targets. For IVDD, previous studies have focused on reducing ROS production or providing cellular antioxidants as therapeutic directions. Plant-derived substances such as genistein, luteoloside, and honokiol markedly reduce the influence of ROS in IVDD progression [16, 26, 36]. Despite the effectiveness of these treatments, concerns persist regarding the safety

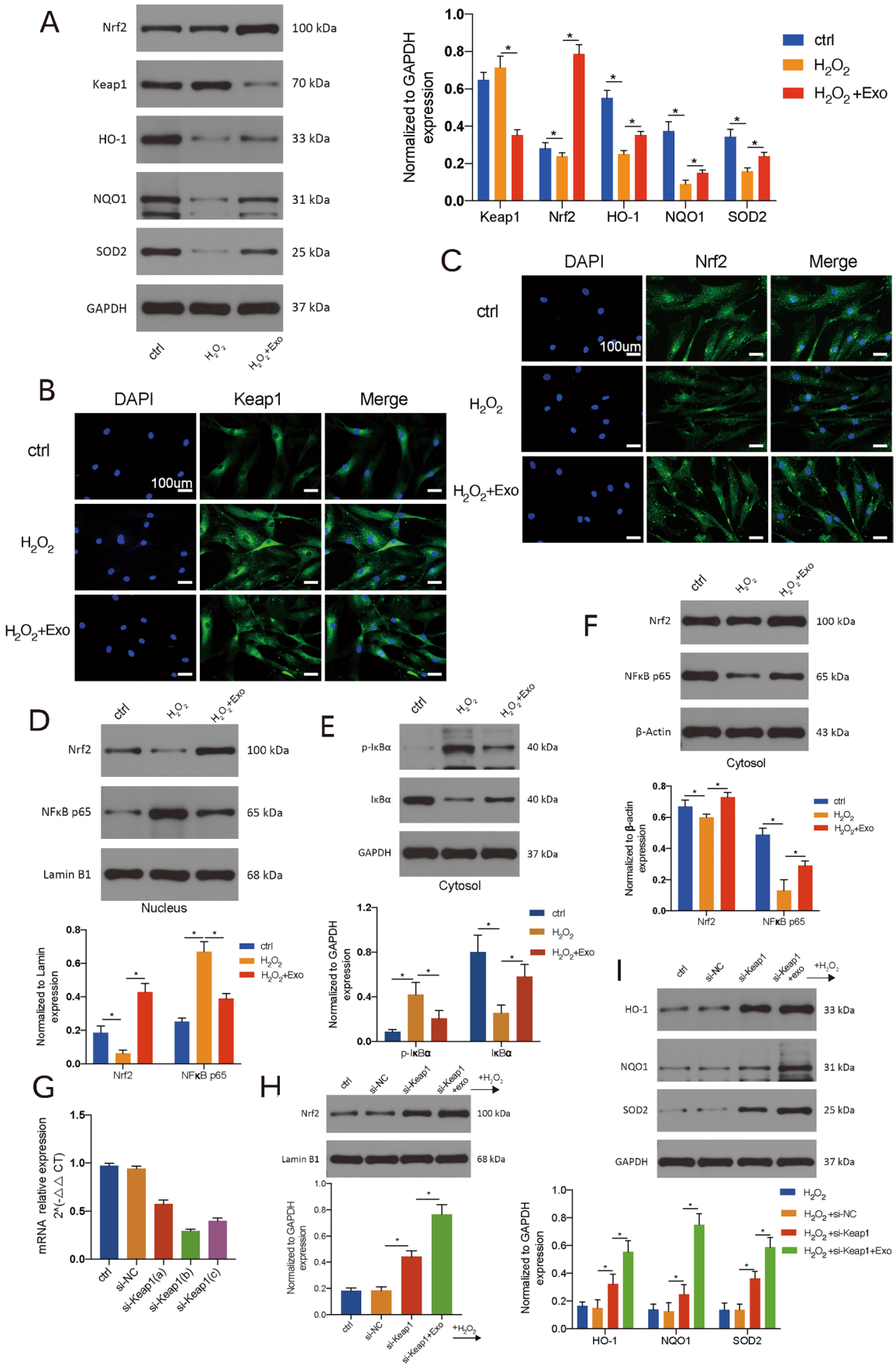
A
Nrf2
Keap1
HO-1
NQO1
SOD2
GAPDH
100 kDa
70 kDa
33 kDa
31 kDa
25 kDa
37 kDa
ctrl
H2O2
H2O2+Exo
Normalized to GAPDH expression
Keap1
Nrf2
HO-1
NQO1
SOD2
B
DAPI
Keap1
Merge
100um
C
Nrf2
D
Lamin B1
68 kDa
Nucleus
Normalized to Lamin expression
NFκB p65
E
p-IκBα
IκBα
40 kDa
Cytosol
Normalized to GAPDH expression
F
β-Actin
43 kDa
Normalized to β-actin expression
G
mRNA relative expression 2^(-△△CT)
si-NC
si-Keap1(a)
si-Keap1(b)
si-Keap1(c)
H
si-Keap1
si-Keap1+exo
+H2O2
si-Keap1+Exo
I
si-Keap1+Exo
H2O2+si-NC
H2O2+si-Keap1
H2O2+si-Keap1+Exo

◂**Fig. 4** BMSC-exos increased the expression and nuclear translocation of Nrf2 and decreased the expression of NF-κB. **a** BMSC-exos reversed the decreased expression of Nrf2 and increased the expression of antioxidant-related proteins (HO-1, NQO1, SOD2). **b** Immunofluorescence of Keap1 in different groups (scale bar, 100 μm). **c** Immunofluorescence of Nrf2 in different groups (scale bar, 100 μm). **d** The protein level of Nrf2 and NF-κB p65 in nucleus using western blot assay in different groups. **e** The protein level of p-IκBα and IκBα in cytosol using western blot assay in different groups. **f** The protein level of Nrf2 and NF-κB p65 in cytosol using western blot assay in different groups. **g** qPCR of mRNA levels of Keap1 after transfected with short interfering RNA. **h** The protein level of Nrf2 in nucleus after transfected with si-Keap1and the enhancement of BMSC-exos towards it. **i** The expression of antioxidant-related protein using western blot assays after treated with si-Keap1 and BMSC-exos. (Data were shown by mean ± SD, $n = 3$, $^*p < 0.05$)

and dosage of the drugs, whether the substance shows other side effects. Further, the specific mechanism of them remains unclear. Finding a safer molecule that activates endogenous antioxidant mechanisms appears to be the key to alleviating disc degeneration. Nrf2 is central to the regulation of antioxidant stress and it may hold promise for the treatment of IVDD.

Different attempts have been made to enhance the endogenous Nrf2 pathway. Compared with small molecule Nrf2 agonists, direct disruption of the Keap1/Nrf2 complex avoids the potential risk of unselected modifications of cysteine residues and can regulate the expression of Nrf2 more rationally and scientifically. Over the past few years, exosomes from stem cells have been found to alleviate intervertebral disc degeneration. This benefit is diverse, enhancing autophagy and reducing apoptosis as well as endoplasmic reticulum stress [37–39]. Given that MSC-derived exosomes can attenuate the systemic inflammatory response caused by sepsis by reducing Keap1expression to enhance the activity of the Nrf2, we wondered whether BMSC-exos have the same beneficial effect on NP cells [25].

In this study, we implemented an NP cell degeneration model using the classical stimulus H_2O_2. Depending on the CCK-8 values at different concentrations, concentrations causing moderate degeneration of NP cells were selected. SA-β-gal staining was then selected to further confirm that cells undergo senescence in response to H_2O_2. In healthy cells, small amount of stress tends to activate the intrinsic antioxidant system. Nuclear translocation of Nrf2 promotes the expression of various antioxidants such as HO-1, NQO1, and SOD2, which are key enzymes responsible for glutathione synthesis [40]. As cells age, in addition to their baseline Nrf2 expression being downregulated, their ability to respond to stress is reduced compared to younger cells [41]. Unexpectedly, the expression of Keap1 and Nrf2 was not significantly different from that of treated NP cells compared with that of H_2O_2-treated cells. The reason may be that H_2O_2 also causes partial stress in the model that simulates degeneration. During the construction of the model, degeneration and oxidative stress are often difficult to separate very specifically. As degeneration and stress are often intertwined, a model of degeneration without stress theoretically does not exist.

Next, we determined whether exosomes mitigate the pathogenesis of IVDD. ROS were significantly decreased in BMSC-exos-treated NP cells. Western blotting showed that BMSC-exos-treated NP cells had a higher antioxidant capacity (higher expression of HO-1, NQO1, and SOD2). Immunofluorescence further confirmed the stronger signal of Nrf2 in the nucleus of NP cells in the BMSC-exos-treated group, suggesting stronger nuclear translocation and antioxidant expression. Inflammation-related molecules (IL-1β, IL-6, TNF-α) are thought to be positively associated with disc degeneration [42]. These inflammatory mediators not only inhibit cell proliferation but also promote apoptosis. MMP13 plays an important role in extracellular matrix remodelling because it promotes the degradation of ECM [43]. Collagen II, which decreases with age, forms an irregular network that keeps proteoglycans and water together and preserves the structural integrity of NP tissue [44, 45]. Additionally, Adamts5 and Aggrecan, which are closely related to IVDD, were evaluated in this study. The dynamic stability of the ECM is then maintained based on the balance of these elements. According to the above results, our results verified that BMSC-exos could reduce inflammation and decrease the degradation of ECM in NP cells.

Because BMSC-exos reduced the expression of inflammation-related genes, we explored the expression of proteins in the NF-κb pathway. H_2O_2 increased the nuclear translocation of NF-κb, and treatment with BMSC-exos suppressed NF-κb expression. We hypothesized that this inhibition by BMSC-exos was related to the activation of Nrf2 signalling, as confirmed in subsequent experiments. According to Bellezza et al., activation of Nrf2/HO-1 inhibited the nuclear translocation of NF-κB by α-TOS [46]. In another report by Bao et al., chlorogenic acid suppressed oxidative stress and inflammation by regulating the Nrf2/HO-1 and NF-κB pathways to prevent diabetic nephropathy [47]. The Nrf2 and NF-κB signalling pathways show much crosstalk. HO-1, a target gene of Nrf2, is the core of Nrf2-mediated NF-κB inhibition. This enzyme catalyses the cleavage of the porphyrin ring to Fe^{2+}, carbon monoxide, and biliverdin, which all contribute to the inhibition of NF-κB transcription [48, 49]. Another refined mechanism relies on the transcription of two signalling pathways in the nucleus. Nrf2 and p65 (the canonical NF-κB subunit) compete for the transcriptional coactivator CBP (CREB-binding protein)-p300 complex, which induces local acetylation of histones, loosening of chromatin structure, and exposure of DNA for assembly of

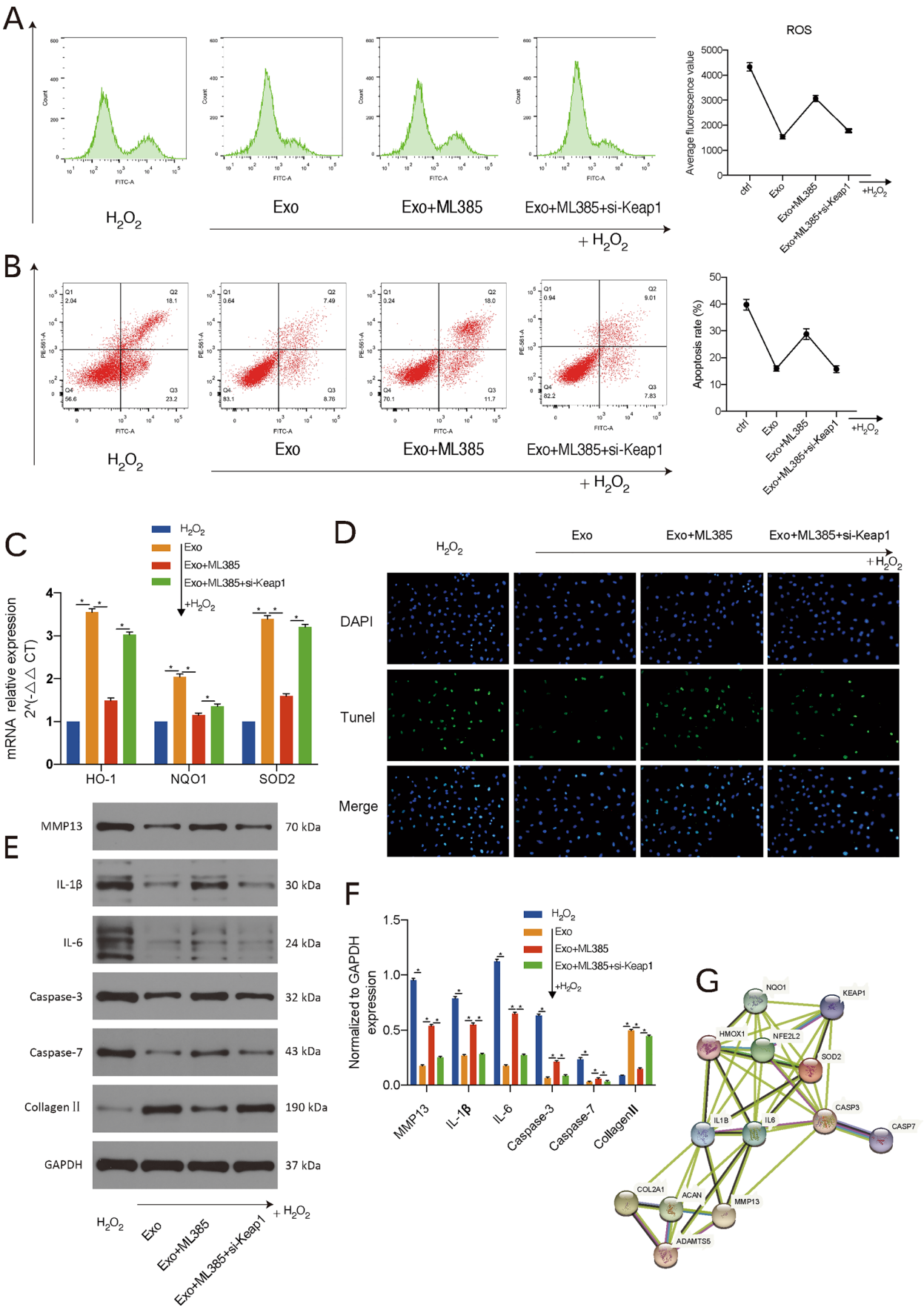
A
ROS
Average fluorescence value
5000
4000
3000
2000
1000
0
ctrl
Exo
Exo+ML385
Exo+ML385+si-Keap1
+H2O2
H2O2
Exo
Exo+ML385
Exo+ML385+si-Keap1
+ H2O2
B
Apoptosis rate (%)
50
40
30
20
10
0
C
H2O2
Exo
Exo+ML385
Exo+ML385+si-Keap1
+H2O2
mRNA relative expression 2^(-△△ CT)
HO-1
NQO1
SOD2
D
H2O2
Exo
Exo+ML385
Exo+ML385+si-Keap1
+H2O2
DAPI
Tunel
Merge
E
MMP13
70 kDa
IL-1β
30 kDa
IL-6
24 kDa
Caspase-3
32 kDa
Caspase-7
43 kDa
Collagen II
190 kDa
GAPDH
37 kDa
H2O2
Exo
Exo+ML385
Exo+ML385+si-Keap1
+ H2O2
F
H2O2
Exo
Exo+ML385
Exo+ML385+si-Keap1
+H2O2
Normalized to GAPDH expression
1.5
1.0
0.5
0.0
MMP13
IL-1β
IL-6
Caspase-3
Caspase-7
CollagenII
G
NQO1
KEAP1
HMOX1
NFE2L2
SOD2
CASP3
IL1B
IL6
CASP7
COL2A1
ACAN
MMP13
ADAMTS5

◂**Fig. 5** Blockage of Nrf2 abrogated the anti-inflammatory, anti-apoptotic, and anti-ECM degradation effects of BMSC-exos under oxidative stress. **a** Flow cytometry of ROS level in different groups. **b** Flow cytometry of apoptosis in different groups. **c** qPCR of mRNA levels of HO-1, NQO1, and SOD2 in each group. **d** Apoptosis of TUNEL staining under different treatments (E-F) The expression of apoptosis, inflammation, and degeneration-related protein under different treatments. **g** Graphical representation of proteins using STRING (https://string-db.org/cgi/input.pl). (Data were shown by mean ± SD, $n = 3$, $^{*}p < 0.05$)

the transcriptional apparatus [48]. Regulating the Nrf2 and NF-κB signalling pathways has been increasingly emphasized in chronic inflammatory diseases such as nephritis, hepatitis, and pneumonia [19, 20, 50]. This research is also the first to report that BMSC-exos enhance the Nrf2 signalling system and inhibit NF-κB signalling in IVDD.

To further validate this pathway, we found that silencing Keap1 mimicked the effect of BMSC-exos treatment and promoted the nuclear shift of Nrf2 and antioxidant expression. BMSC-exos synergistically enhanced the silencing effect of Keap1. Next, we interfered with Nrf2 expression to observe whether BMSC-exos exert their anti-inflammatory, apoptosis-reducing, and ECM degradation-reducing effects through the Nrf2 pathway. ML385 is a proven Nrf2-specific inhibitor that inhibits the expression of downstream genes by binding to the Neh1 domain of Nrf2 [51]. We considered the group cotreated with H_2O_2 and BMSC-exos as a negative control and found that the anti-inflammatory, apoptosis-reducing, and ECM degradation-reducing abilities of exosomes were significantly reduced after using ML385 to specifically inhibit the effects of Nrf2. Not surprisingly, after silencing Keap1 again, these benefits of BMSC-exos were restored. Based on the above findings, BMSC-exos improved the antioxidant capacity of NP cells and slowed the degenerative process, at least partially through the Keap1/Nrf2 signalling pathway.

The in vitro results reaffirmed our study. We used traditional acupuncture to mimic IVDD in a rat model [52]. AAV vectors transfer target genes in vivo due to their high safety and low immunogenicity [5]. The observed volume reduction of NP tissue and prolonged downregulation of antioxidants in the BMSC-exos and aav-si-Nrf2 cotreated groups indicated that BMSC-exos at least partially functioned by communicating with Nrf2. The opposite results were obtained when intervening in keap1 again, proving that Keap1 was upstream of Nrf2.

MSC-exos present considerable prospects in nanomedicine considering their attractive biological properties and impressive therapeutic potential for inflammatory and degenerative diseases [24, 25, 53]. Although studies have reported that MSC-exos promote Nrf2 expression in macrophages and vascular endothelial cells, no report has investigated the effects and potential mechanisms of MSC-exos communicating with Nrf2 signalling in IVDD [25, 54]. In the present study, our results demonstrate the major role of BMSC-exos in regulating the Keap1/Nrf2 pathway in degenerating discs. The decrease in ROS also reduces inflammation, decreases apoptosis, and inhibits matrix degradation. Current evidences suggest that many noncoding RNAs, such as miRNAs and long noncoding RNAs, are present in exosomes and that they are involved in regulating cellular life activities [22, 23]. In Xie, Shi, and Yang's reports, BMSC-exos contained abundant miR-200a and miR-23a [55, 56]. These two miRNAs bind to the 3′-UTR of Keap1 and repress the transcription of Keap1 in other disease models [54, 57]. The redox miRNAs that target Keap1 may explain why BMSC-exos increased Nrf2 expression in target cells, but further experiments are warranted to validate this hypothesis in NP cells.

In this research, we found BMSC-exos could reduce ROS in degenerated NP cells by regulating the Keap1/Nrf2 axis. However, if it were to be translatable to the human experience, BMSC-exos may not be as efficient as it were in rat model. Human intervertebral discs bear more load than those in rat tails. There might be more ROS in human intervertebral discs than rats, which required stronger antioxidants. So, although still in its infancy, engineered exosomes that target Keap1 or Nrf2 may be a translational direction in the human experience, as they are more precise in targeting NP cells and more efficient in activating antioxidant pathways.

One limitation of this study is that although the rat model applied in our studies is widely used in intervertebral disc disorders, differences persist in the biomechanical properties compared with large animals such as pigs, goats, and monkeys. Rodents may undergo different IVDD processes compared with mammals. Besides, the cells in rat discs are rich in notochordal cells, while there are barely no notochordal cells present in the human discs. Further, the structures of the discs in human and rats are quite different in terms of relative thickness of endplate, diffusion patterns. At last, besides anti-ROS effects, future therapeutic strategies for IVDD may also need to address synergistic therapeutic effects of pro-anabolic factors.

Conclusion

Nrf2 and NF-κB are two key pathways regulating the exquisite balance of the cellular redox status and response to stress and inflammation. We demonstrate for the first time that BMSC-exos can exert their ROS-reducing role by regulating the Keap1/Nrf2 pathway and suppressing NF-κB signalling in NP cells stimulated by H_2O_2. Exuberant expression of antioxidative proteins mediated by Nrf2 nuclear

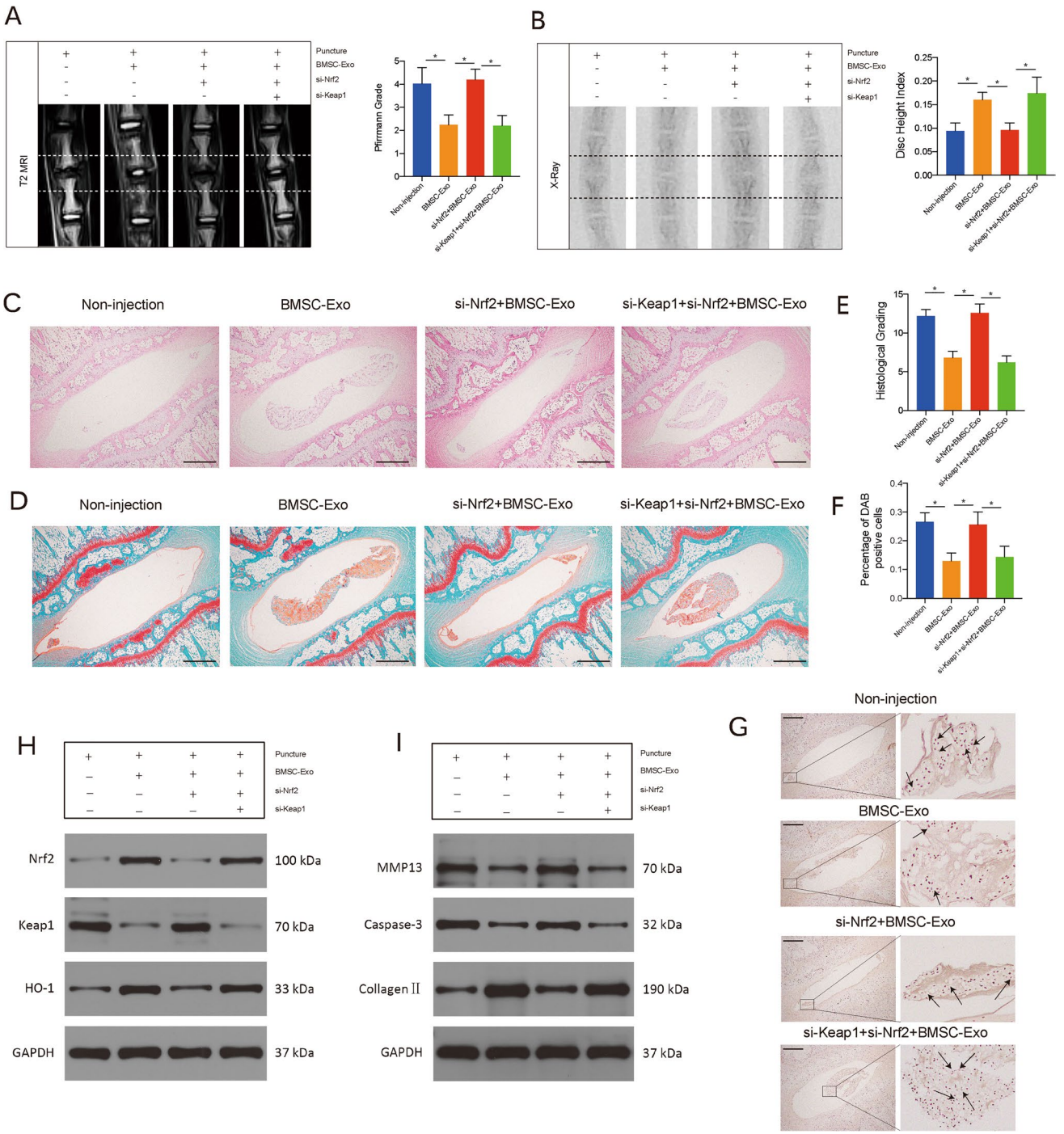

Fig. 6 BMSC-exos activates Nrf2 in vivo to alleviate IVDD in a rat model. **a** Evaluation of rat tails in different groups using a 3.0T MR based on Pfirrmann grade. **b** Evaluation of rat tails in different groups using X-rays based on disc height index (DHI). **c** HE staining of discs under different treatments (scale bar, 1,000 μm). **d** Safranin-O staining of discs under different treatments (scale bar, 1,000 μm). **e** Histological grade of intervertebral discs in different groups. **f**-**g** TUNEL staining of intervertebral discs in different groups (scale bar, 1,000 μm). Arrows indicated DAB positive cells. **h** The expression of Keap1, Nrf2, and HO-1 in NP tissue in different groups.**i** The expression of MMP13, Caspase-3, and Collagen II in NP tissue in different groups. (Data were shown by mean ± SD, $n = 3$, $^*p < 0.05$)

translocation restrained apoptosis and reduced inflammation and ECM degeneration. Together, these three key molecular events alleviated the cellular and histological response to oxidative stress in IVDD progression. In the future, engineered exosomes therapy that targets Keap1 or Nrf2 may be a new treatment for IVDD.

Abbreviations *BMSC-exos*: Bone marrow mesenchymal stem cell derived exosomes; *DAPI*: 4′,6-diamidino-2-phenylindole; *DHI*: Disc height index; *DMEM*: Dulbecco's modified Eagle's medium; *ECM*: Extracellular matrix; *FBS*: Foetal bovine serum; *HO-1*: Heme-oxygenase-1; *IVDD*: Intervertebral disc degeneration; *Keap1*: Kelch-like ECH-associated protein 1; *NP*: Nucleus pulposus; *NQO1*: NADP(H) quinone oxidoreductase 1; *Nrf2*: Transcription factor nuclear factor erythroid-2 related factor 2; *ROS*: Reactive oxygen species; *SODs*: Superoxide dismutases; *TEM*: Transmission electron microscopy; *8-OHdG*: 8-Hydroxy-1,2 deoxyguanosine

Supplementary Information The online version contains supplementary material available at https://doi.org/10.1007/s12015-023-10570-w.

Acknowledgements We thanked Professor Mingxia Fan, the director of Key Laboratory of Magnetic Resonance, East China Normal University, for her help in the MRI of rat tails.

Authors' Contributions JS, JYJ, HLW, FZ designed the experiments. GYX, XL, SYL, YXZ, SX and FZ performed the experiments and acquired the data. GYX, XL, XLX and XSM analysed the data. GYX, SYL and FZL supervised the project and wrote the manuscript.

Funding This work was supported by Shanghai Sailing Program, Shanghai, China (20YF1429900); National Natural Science Foundation of China, China (81972093, 81972109, 82102620, 82172490 and 82272549).

Data Availability The data underlying this article will be shared on reasonable request to the corresponding author.

Code Availability Not applicable.

Declarations

Ethics Approval The study was approved by the Ethics Committee of Huashan Hospital, Fudan University (2022-042) and the procedures followed were in accordance with the Helsinki Declaration.

Consent to Participate The nucleus pulposus tissue were collected after obtaining informed consent from the donors.

Consent for Publication All authors consented to publish this paper.

Conflict of Interest The authors declare that they have no conflict of interest in the authorship.

References

1. Hoy, D. G., Smith, E., Cross, M., et al. (2014). The global burden of musculoskeletal conditions for 2010: An overview of methods. *Annals of the Rheumatic Diseases, 73*, 982–989.
2. Luoma, K., Riihimaki, H., Luukkonen, R., Raininko, R., Viikari-Juntura, E., & Lamminen, A. (2000). Low back pain in relation to lumbar disc degeneration. *Spine (Phila Pa 1976), 25*, 487–492.
3. Walker, M. H., & Anderson, D. G. (2004). Molecular basis of intervertebral disc degeneration. *The Spine Journal: Official Journal of the North American Spine Society, 4*, 158S-166S.
4. Dowdell, J., Erwin, M., Choma, T., Vaccaro, A., Iatridis, J., & Cho, S. K. (2017). Intervertebral disk degeneration and repair. *Neurosurgery, 80*, S46–S54.
5. Song, J., Chen, Z. H., Zheng, C. J., et al. (2020). Exosome-transported circRNA_0000253 competitively Adsorbs MicroRNA-141-5p and increases IDD. *Molecular Therapy Nucleic Acids, 21*, 1087–1099.
6. Song, J., Wang, H. L., Song, K. H., et al. (2018). CircularRNA_104670 plays a critical role in intervertebral disc degeneration by functioning as a ceRNA. *Experimental & Molecular Medicine, 50*, 1–12.
7. Feng, C., Yang, M., Lan, M., et al. (2017). ROS: Crucial intermediators in the pathogenesis of intervertebral disc degeneration. *Oxidative Medicine and Cellular Longevity, 2017*, 5601593.
8. Suzuki, S., Fujita, N., Hosogane, N., et al. (2015). Excessive reactive oxygen species are therapeutic targets for intervertebral disc degeneration. *Arthritis Research & Therapy, 17*, 316.
9. Poveda, L., Hottiger, M., Boos, N., & Wuertz, K. (2009). Peroxynitrite induces gene expression in intervertebral disc cells. *Spine (Phila Pa 1976), 34*, 1127–1133.
10. Bellezza, I., Giambanco, I., Minelli, A., & Donato, R. (2018). Nrf2-Keap1 signaling in oxidative and reductive stress. *Biochimica et Biophysica Acta - Molecular Cell Research, 1865*, 721–733.
11. Tonelli, C., Chio, I. I. C., & Tuveson, D. A. (2018). Transcriptional regulation by Nrf2. *Antioxidants & Redox Signaling, 29*, 1727–1745.
12. Cullinan, S. B., Gordan, J. D., Jin, J., Harper, J. W., & Diehl, J. A. (2004). The Keap1-BTB protein is an adaptor that bridges Nrf2 to a Cul3-based E3 ligase: Oxidative stress sensing by a Cul3-Keap1 ligase. *Molecular and Cellular Biology, 24*, 8477–8486.
13. Keleku-Lukwete, N., Suzuki, M., & Yamamoto, M. (2018). An overview of the Advantages of KEAP1-NRF2 system activation during Inflammatory Disease Treatment. *Antioxidants & Redox Signaling, 29*, 1746–1755.
14. Ma, Q. (2013). Role of nrf2 in oxidative stress and toxicity. *Annual Review of Pharmacology and Toxicology, 53*, 401–426.
15. Zelko, I. N., Mariani, T. J., & Folz, R. J. (2002). Superoxide dismutase multigene family: A comparison of the CuZn-SOD (SOD1), Mn-SOD (SOD2), and EC-SOD (SOD3) gene structures, evolution, and expression. *Free Radical Biology and Medicine, 33*, 337–349.
16. Lin, J., Chen, J., Zhang, Z., et al. (2019). Luteoloside inhibits IL-1beta-Induced apoptosis and catabolism in nucleus pulposus cells and ameliorates intervertebral disk degeneration. *Frontiers in Pharmacology, 10*, 868.
17. Luo, X., Huan, L., Lin, F., et al. (2021). Ulinastatin ameliorates IL-1beta-induced cell dysfunction in human nucleus pulposus cells via Nrf2/NF-kappaB pathway. *Oxidative Medicine and Cellular Longevity, 2021*, 5558687.
18. Wang, K., Hu, S., Wang, B., Wang, J., Wang, X., & Xu, C. (2019). Genistein protects intervertebral discs from degeneration via Nrf2-mediated antioxidant defense system: An in vitro and in vivo study. *Journal of Cellular Physiology*. https://doi.org/10.1002/jcp.28301
19. Lu, M. C., Zhao, J., Liu, Y. T., et al. (2019). CPUY192018, a potent inhibitor of the Keap1-Nrf2 protein-protein interaction, alleviates renal inflammation in mice by restricting oxidative stress and NF-kappaB activation. *Redox Biology, 26*, 101266.
20. Xu, J., Li, H. B., Chen, L., et al. (2019). BML-111 accelerates the resolution of inflammation by modulating the Nrf2/HO-1 and NF-kappaB pathways in rats with ventilator-induced lung injury. *International Immunopharmacology, 69*, 289–298.
21. Wang, T., Jian, Z., Baskys, A., et al. (2020). MSC-derived exosomes protect against oxidative stress-induced skin injury via adaptive regulation of the NRF2 defense system. *Biomaterials, 257*, 120264.
22. Valadi, H., Ekstrom, K., Bossios, A., Sjostrand, M., Lee, J. J., & Lotvall, J. O. (2007). Exosome-mediated transfer of mRNAs and microRNAs is a novel mechanism of genetic exchange between cells. *Nature Cell Biology, 9*, 654–659.
23. Wortzel, I., Dror, S., Kenific, C. M., & Lyden, D. (2019). Exosome-mediated metastasis: Communication from a distance. *Developmental Cell, 49*, 347–360.
24. Xian, P., Hei, Y., Wang, R., et al. (2019). Mesenchymal stem cell-derived exosomes as a nanotherapeutic agent for amelioration of

inflammation-induced astrocyte alterations in mice. *Theranostics, 9*, 5956–5975.
25. Shen, K., Jia, Y., Wang, X., et al. (2021). Exosomes from adipose-derived stem cells alleviate the inflammation and oxidative stress via regulating Nrf2/HO-1 axis in macrophages. *Free Radical Biology and Medicine, 165*, 54–66.
26. Xia, C., Zeng, Z., Fang, B., et al. (2019). Mesenchymal stem cell-derived exosomes ameliorate intervertebral disc degeneration via anti-oxidant and anti-inflammatory effects. *Free Radical Biology and Medicine, 143*, 1–15.
27. Issy, A. C., Castania, V., Castania, M., et al. (2013). Experimental model of intervertebral disc degeneration by needle puncture in Wistar rats. *Brazilian Journal of Medical and Biological Research, 46*, 235–244.
28. Frapin, L., Clouet, J., Delplace, V., Fusellier, M., Guicheux, J., & Le Visage, C. (2019). Lessons learned from intervertebral disc pathophysiology to guide rational design of sequential delivery systems for therapeutic biological factors. *Advanced Drug Delivery Reviews, 149–150*, 49–71.
29. Sun, J. C., Zheng, B., Sun, R. X., et al. (2019). MiR-499a-5p suppresses apoptosis of human nucleus pulposus cells and degradation of their extracellular matrix by targeting SOX4. *Biomedicine & Pharmacotherapy, 113*, 108652.
30. Li, Z., Li, X., Chen, C., Chan, M. T. V., Wu, W. K. K., & Shen, J. (2017). Melatonin inhibits nucleus pulposus (NP) cell proliferation and extracellular matrix (ECM) remodeling via the melatonin membrane receptors mediated PI3K-Akt pathway. *Journal of Pineal Research.* https://doi.org/10.1111/jpi.12435
31. Dimozi, A., Mavrogonatou, E., Sklirou, A., & Kletsas, D. (2015). Oxidative stress inhibits the proliferation, induces premature senescence and promotes a catabolic phenotype in human nucleus pulposus intervertebral disc cells. *European Cells & Materials, 30*, 89–102. discussion 103.
32. D'Autreaux, B., & Toledano, M. B. (2007). ROS as signalling molecules: Mechanisms that generate specificity in ROS homeostasis. *Nature Reviews Molecular Cell Biology, 8*, 813–824.
33. Madreiter-Sokolowski, C. T., Thomas, C., & Ristow, M. (2020). Interrelation between ROS and ca(2+) in aging and age-related diseases. *Redox Biology, 36*, 101678.
34. Yamamoto, M., Kensler, T. W., & Motohashi, H. (2018). The KEAP1-NRF2 system: A thiol-based sensor-effector apparatus for maintaining redox homeostasis. *Physiological Reviews, 98*, 1169–1203.
35. Labrousse-Arias, D., Martinez-Ruiz, A., & Calzada, M. J. (2017). Hypoxia and redox signaling on extracellular matrix remodeling: From mechanisms to pathological implications. *Antioxidants & Redox Signaling, 27*, 802–822.
36. Tang, P., Gu, J. M., Xie, Z. A., et al. (2018). Honokiol alleviates the degeneration of intervertebral disc via suppressing the activation of TXNIP-NLRP3 inflammasome signal pathway. *Free Radical Biology and Medicine, 120*, 368–379.
37. Cheng, X., Zhang, G., Zhang, L., et al. (2018). Mesenchymal stem cells deliver exogenous miR-21 via exosomes to inhibit nucleus pulposus cell apoptosis and reduce intervertebral disc degeneration. *Journal of Cellular and Molecular Medicine, 22*, 261–276.
38. Liao, Z., Luo, R., Li, G., et al. (2019). Exosomes from mesenchymal stem cells modulate endoplasmic reticulum stress to protect against nucleus pulposus cell death and ameliorate intervertebral disc degeneration in vivo. *Theranostics, 9*, 4084–4100.
39. Luo, L., Jian, X., Sun, H., et al. (2021). Cartilage endplate stem cells inhibit intervertebral disc degeneration by releasing exosomes to nucleus pulposus cells to activate Akt/autophagy. *Stem Cells, 39*, 467–481.
40. Lu, S. C. (2009). Regulation of glutathione synthesis. *Molecular Aspects of Medicine, 30*, 42–59.
41. Zhang, H., Davies, K. J. A., & Forman, H. J. (2015). Oxidative stress response and Nrf2 signaling in aging. *Free Radical Biology and Medicine, 88*, 314–336.
42. Sakai, D., & Grad, S. (2015). Advancing the cellular and molecular therapy for intervertebral disc disease. *Advanced Drug Delivery Reviews, 84*, 159–171.
43. Ortega, N., Behonick, D., Stickens, D., & Werb, Z. (2003). How proteases regulate bone morphogenesis. *Annals of the New York Academy of Sciences, 995*, 109–116.
44. Deng, H., Huang, X., & Yuan, L. (2016). Molecular genetics of the COL2A1-related disorders. *Mutation Research - Reviews in Mutation Research, 768*, 1–13.
45. Colombier, P., Clouet, J., Hamel, O., Lescaudron, L., & Guicheux, J. (2014). The lumbar intervertebral disc: From embryonic development to degeneration. *Joint, Bone, Spine: Revue Du Rhumatisme, 81*, 125–129.
46. Bellezza, I., Tucci, A., Galli, F., et al. (2012). Inhibition of NF-kappaB nuclear translocation via HO-1 activation underlies alpha-tocopheryl succinate toxicity. *Journal of Nutritional Biochemistry, 23*, 1583–1591.
47. Bao, L., Li, J., Zha, D., et al. (2018). Chlorogenic acid prevents diabetic nephropathy by inhibiting oxidative stress and inflammation through modulation of the Nrf2/HO-1 and NF-kB pathways. *International Immunopharmacology, 54*, 245–253.
48. Wardyn, J. D., Ponsford, A. H., & Sanderson, C. M. (2015). Dissecting molecular cross-talk between Nrf2 and NF-kappaB response pathways. *Biochemical Society Transactions, 43*, 621–626.
49. Ahmed, S. M., Luo, L., Namani, A., Wang, X. J., & Tang, X. (2017). Nrf2 signaling pathway: Pivotal roles in inflammation. *Biochimica et Biophysica Acta - Molecular Basis of Disease, 1863*, 585–597.
50. Zhao, X. J., Yu, H. W., Yang, Y. Z., et al. (2018). Polydatin prevents fructose-induced liver inflammation and lipid deposition through increasing miR-200a to regulate Keap1/Nrf2 pathway. *Redox Biology, 18*, 124–137.
51. Singh, A., Venkannagari, S., Oh, K. H., et al. (2016). Small molecule inhibitor of NRF2 selectively intervenes therapeutic resistance in KEAP1-Deficient NSCLC tumors. *ACS Chemical Biology, 11*, 3214–3225.
52. Zhang, H., La Marca, F., Hollister, S. J., Goldstein, S. A., & Lin, C. Y. (2009). Developing consistently reproducible intervertebral disc degeneration at rat caudal spine by using needle puncture. *Journal of Neurosurgery. Spine, 10*, 522–530.
53. Mager, S. E. L. A., Breakefield, I., & Wood, X. O. (2013). Extracellular vesicles: Biology and emerging therapeutic opportunities. *Nature Reviews. Drug Discovery, 12*, 347–357.
54. Chen, B., Sun, Y., Zhang, J., et al. (2019). Human embryonic stem cell-derived exosomes promote pressure ulcer healing in aged mice by rejuvenating senescent endothelial cells. *Stem Cell Research & Therapy, 10*, 142.
55. Xie, L., Chen, Z., Liu, M., et al. (2020). MSC-derived exosomes protect vertebral endplate chondrocytes against apoptosis and calcification via the miR-31-5p/ATF6 Axis. *Molecular Therapy Nucleic Acids, 22*, 601–614.
56. Shi, Q. Z., Yu, H. M., Chen, H. M., Liu, M., & Cheng, X. (2021). Exosomes derived from mesenchymal stem cells regulate Treg/Th17 balance in aplastic anemia by transferring miR-23a-3p. *Clinical and Experimental Medicine*. https://doi.org/10.1007/s10238-021-00701-3
57. Zimta, A. A., Cenariu, D., & Irimie, A. (2019). The role of Nrf2 activity in cancer development and progression. *Cancers (Basel)*. https://doi.org/10.3390/cancers11111755